OPEN

Histidine-Rich Glycoprotein Suppresses Hyperinflammatory Responses of Lung in a Severe Acute Pancreatitis Mouse Model

Kinya Terao, MD,* Hidenori Wake, PhD,* Naoto Adachi, MD, PhD,* Keyue Liu, MD, PhD,*
Kiyoshi Teshigawara, PhD,* Hideo Takahashi, MD, PhD,†
Shuji Mori, PhD,‡ and Masahiro Nishibori, MD, PhD*

Objectives: Severe acute pancreatitis is a highly lethal disease caused by systemic inflammatory response syndrome, leading to multiple organ failure. We recently showed that histidine-rich glycoprotein (HRG) supplemental therapy ameliorated septic acute respiratory distress syndrome due to unnecessary neutrophil activation and immunothrombosis formation. Here, we evaluated the effect of HRG on lung inflammation followed by pancreatitis in a severe acute pancreatitis mouse model.

Methods: Mice received intraperitoneal injections of cerulein 7 times (100 μg/kg each) at 1-hour intervals to induce acute pancreatitis. Immediately after the first cerulein injection, phosphate-buffered saline, human serum albumin (20 mg/kg), or HRG (20 mg/kg) was intravenously injected. One hour after the last cerulein injection, phosphate-buffered saline or lipopolysaccharide (5 mg/kg) was intravenously injected into the tail vein. We evaluated lung inflammatory level after pancreatitis.

Results: We observed significantly decreased plasma HRG levels in an acute pancreatitis mouse model. Histidine-rich glycoprotein treatment inhibited lung edema and the accumulation of neutrophil in severe acute pancreatitis, but HRG did not directly affect pancreatitis. Moreover, HRG suppressed tumor necrosis factor α, inducible nitric oxide synthase, interleukin 6, and neutrophil elastase mRNA expression and myeloperoxidase activity in the lung.

Conclusions: These data suggested that HRG ameliorated lung inflammation secondary to pancreatitis.

Key Words: histidine-rich glycoprotein, severe acute pancreatitis, acute respiratory distress syndrome

(*Pancreas* 2018;47: 1156–1164)

Acute pancreatitis is an acute abdominal disease caused by an excess intake of alcohol, hyperlipidemia, or cholelithiasis.[1,2] Although premature activation of digestive enzymes is the first step in acute pancreatitis, inflammatory reactions provoke general symptoms.[1–3] The facilitation of vascular permeability leads to an extravasation of plasma, a decrease in circulating blood volume, and thus circulatory distress.[1,2] The activation of neutrophils plays a crucial role in the development of systemic inflammatory response syndrome caused by acute pancreatitis.[4–6] Bacterial infection is a serious complication of acute pancreatitis, which leads to acute lung injury, acute kidney injury, and multiple organ failure with high morbidity and mortality.[7–10]

Histidine-rich glycoprotein (HRG) is a 75-kDa plasma glycoprotein, which is produced in the liver and secreted to the whole body.[11–13] It binds to various substances and shows pharmacological activity, such as antimicrobial,[14–17] antiangiogenic,[18–20] anticoagulation,[21,22] and antifibrinolysis activity.[23,24] In our previous study, in which we investigated the effects of HRG on neutrophil functions, HRG facilitated the passage of neutrophils through microvessels by changing their shape, and it prevented the unnecessary activation of neutrophils.[6]

Because neutrophil adhesion to the inflammatory site is the first step in the development of acute respiratory distress syndrome secondary to pancreatitis, in the present study we examined the effects of HRG on neutrophil functions by using an animal model of pancreatitis induced by cerulein. We also applied lipopolysaccharide (LPS) to evaluate acute lung injury, which is a life-threatening complication of systemic inflammatory response syndrome after acute pancreatitis.

MATERIALS AND METHODS

Reagents

Human serum albumin (HSA), phosphate-buffered saline (PBS), cerulein and LPS (*Escherichia coli* O55:B5) were purchased from Sigma-Aldrich (St Louis, Mo). Rat-derived antimouse Gr-1 fluorescein isothiocyanate was purchased from eBioscience (San Diego, Calif). Rabbit-derived antihuman HRG polyclonal antibody was created in our laboratory. Goat-derived antirabbit IgG antibody was purchased from MBL (Nagoya, Japan). D-Phenylalanyl-arginyl chloromethyl ketone was purchased from Cayman Chemical (Ann Arbor, Mich). Aprotinin, leupeptin, and benzylsulfonyl fluoride was purchased from Wako Pure Chemical Industries (Osaka, Japan). Nafamostat mesylate was purchased from Tokyo Chemical Industry (Tokyo, Japan). Benzamidine hydrochloride was purchased from nacalai tesque (Kyoto, Japan).

Animals

This study was approved by the Committee on Animal Experimentation at Okayama University School of Medicine, Dentistry

and Pharmaceutical Sciences, Okayama, Japan. All animals were cared for in compliance with the Principles of Laboratory Animal Care formulated by Okayama University School of Medicine, Dentistry and Pharmaceutical Sciences. Male C57BL/6N mice at 8 to 9 weeks of age weighing 22 to 25 g were purchased from Japan SLC (Shizuoka, Japan).

The animals were housed in a temperature-controlled room at 23°C and maintained in an alternating 12-hour light/12-hour dark cycle (lights on at 6:00 A.M.). A certified diet and water were provided ad libitum. Animals were deprived of food for 12 hours preceding the start of experiments.

Cerulein-Induced Acute Pancreatitis With Endotoxemia

Mice were randomly allocated to 1 of the following 6 groups: sham, cerulein, LPS, cerulein + LPS + PBS, cerulein + LPS + HSA, or cerulein + LPS + HRG. The animals received intraperitoneal injections of cerulein 7 times (100 μg/kg each) at 1-hour intervals to induce acute pancreatitis. Immediately after the first cerulein injection, PBS or HSA (20 mg/kg) or HRG (20 mg/kg) was intravenously injected into the tail vein. One hour after the last cerulein injection, PBS or LPS (5 mg/kg) was intravenously
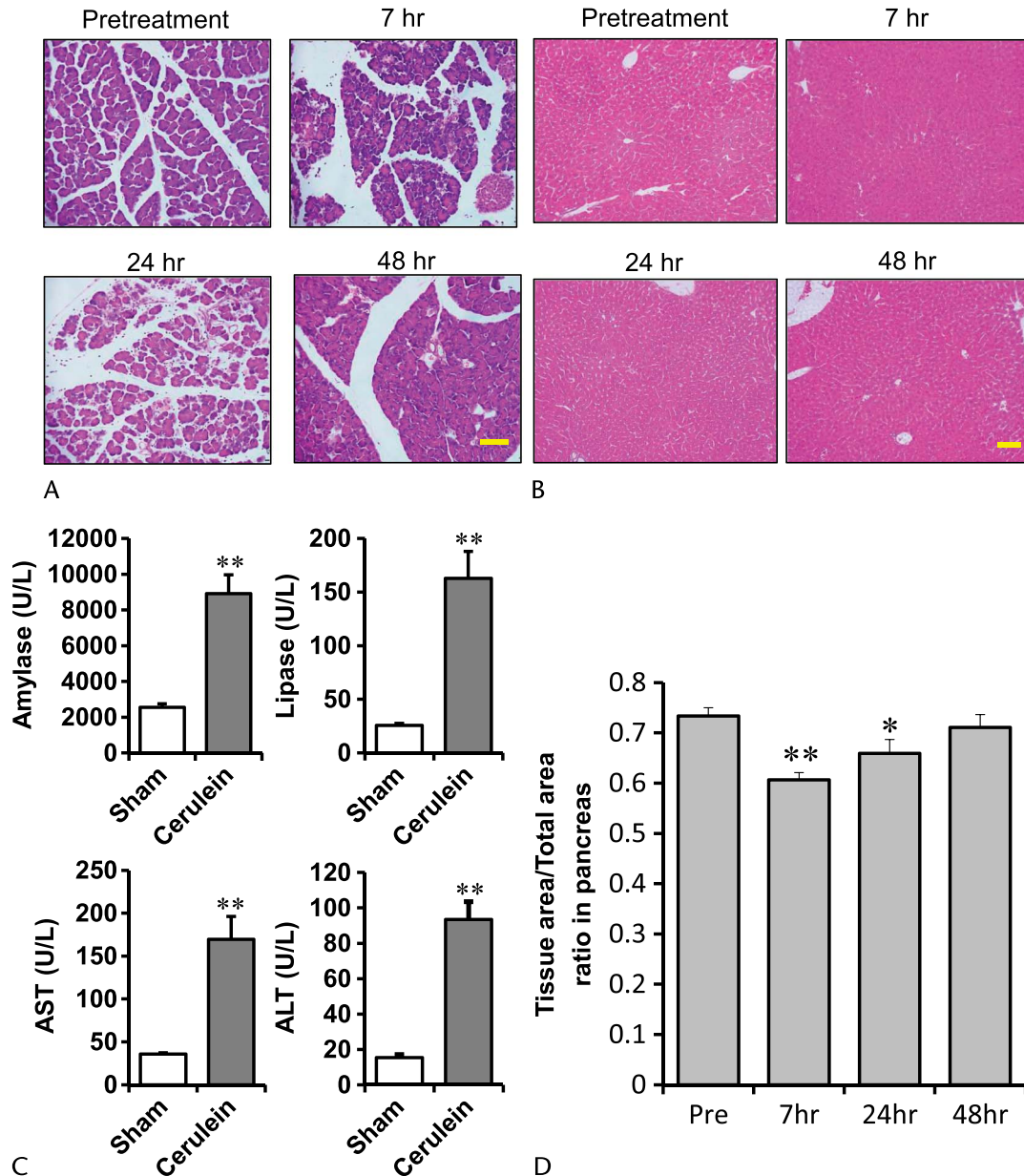
FIGURE 1. Typical photographs showing the pancreas and the liver by HE stain and the plasma concentrations of pancreatic and hepatic enzymes. A (pancreas), B (liver), before treatment and 7, 24, and 48 hours after the first cerulein injection. Cerulein was injected 7 times (100 μg/kg each). Scale bars, 100 μm. C, Serum concentrations of amylase, lipase, AST (aspartate animostransferase), and ALT (alanine animostransferase) at 7 hours after the first injection. **$P < 0.01$ vs sham. The results are presented as mean ± SEM of 5 mice. D, Tissue area/total area ratio in pancreas pretreatment and 7, 24, and 48 hours after the first cerulein injection. *$P < 0.05$ and **$P < 0.01$ vs sham. The results are presented as mean ± SEM of 5 mice.

injected into the tail vein. Mice were killed 7, 11, 24, or 48 hours after the first injection of cerulein depending on experiments.

Purification of HRG From Human Plasma

Human HRG was purified in our laboratory from human plasma supplied by the Japanese Red Cross Society. D-Phenylalanyl-arginyl chloromethyl ketone, aprotinin, leupeptin, benzylsulfonyl fluoride, benzamidine hydrochloride, and nafamostat mesylate as protease inhibitors were added to the human plasma, and the mixture was centrifuged twice at 10,000 rpm at 4°C. The supernatant was incubated with nickel-nitrilotriacetic acid agarose gel (Qiagen, Hilden, Germany) while being gently mixed for 2 hours at 4°C. The gel was then transferred into a column and washed with 50 mM imidazole in 10 mM Tris-buffered saline (TBS) (pH 8.0), 2 M NaCl in 10 mM TBS (pH 8.0), and 100 mM imidazole in 10 mM TBS (pH 8.0). Histidine-rich glycoprotein was eluted by 300 mM imidazole in 10 mM TBS (pH 8.0) from the gel. The extract was then loaded into a Mono Q column (GE Healthcare, Little Chalfont, United Kingdom) and further purified by NaCl gradient. The purified HRG was identified and collected by sodium dodecyl sulfate-polyacrylamide gel electrophoresis using a western blot with antihuman HRG polyclonal antibody. The obtained human HRG was stored at −80°C.

Serum Concentrations of Amylase and Lipase

Seven hours after the first cerulein injection, mice were killed and blood samples were collected from the right ventricle. The samples were centrifuged at 12,000 g at 4°C, and serum concentrations of amylase and lipase were determined according to routine laboratory procedures by SRL (Tokyo, Japan).

Myeloperoxidase Activity of Mouse Lung Tissue

Twenty-four hours after the first cerulein injection, mice were killed and all lung tissue were harvested, quickly homogenized with the assay buffer and centrifuged at 12,000 g for 10 minutes at 4°C. The supernatants were collected and stored at −80°C. The myeloperoxidase activity in the supernatants was assayed using an myeloperoxidase (MPO) assay kit (Abcam, Cambridge, Mass) according to the manufacturer's instructions. Each value represents the relative level of that in the sham group.

Immunohistochemistry

Twenty-four hours after the first cerulein injection, blood was removed from mice of each group. Mice were killed and the upper lobes of the left lung were collected and fixed in 10% buffered formalin. The fixed lung was embedded in paraffin, and immunohistochemical staining for Gr-1 was performed on 5-μm sections with fluorescein isothiocyanate–labeled rat-derived antimouse Gr-1 monoclonal antibody (5 μg/mL) for 2 hours at room temperature. Gr-1–positive neutrophils were counted in the lung section at ×400 magnification under a fluorescent microscope.

Real-Time Quantitative Polymerase Chain Reaction

Eleven hours after the first cerulein injection, mice were killed and a part of the left lung was collected and immediately stored in RNAlater (Thermo Fisher, Waltham, Mass). Total RNA was extracted using an RNeasy Mini kit (Qiagen). Complementary DNA was synthesized with a Takara RNA polymerase chain reaction (PCR) kit, Version 3.0 (TAKARA BIO, Nagahama, Japan). cDNA was mixed with SYBR premix Ex Taq (TAKARA BIO) and sequence-specific primers. Real-time PCR reactions were performed with a LightCycler (Roche, Basel, Switzerland)

according to the manufacturer's instruction. PCR amplification products were analyzed by a melting curve to ascertain the specificity of amplification. GAPDH expression was used to normalize cDNA levels.

Primer Sequence for Real-Time PCR

Inducible nitric oxide synthase (iNOS) (NM010927) F-5′ GAT TTT GCA TGA CAC TCT TCA 3′, R-5′ GGA GCC ATA ATA CTG GTT GAT 3′; tumor necrosis factor α (TNF-α) (NM013693) F-5′ GAC CCT CAC ACT CAG ATC ATC CTT CT 3′, R-5′ GCG CTG GCT CAG CCA CTC 3′; interleukin 6 (IL-6) (NM031168) F-5′ GAC CTG TCT ATA CCA CTT CAC A 3′, R-5′ CTC TGG AAG TTT CAG ATT GTT 3′; neutrophil elastase (NM015779) F-5′ CTA CTG GCA TTG TTC CTG GGT G 3′, R-5′ GCT GAC ATG ACG AAG TTC CTG G 3′; glyceraldehyde-3-phosphate dehydrogenase (GAPDH) (NM008084) F-5′ TGA CGT GCC GCC TGG AGA AA 3′, R-5′ AGT GTA GCC CAA GAT GCC CTT CAG 3′

FIGURE 2. Changes in plasma levels of HRG in cerulein-induced pancreatitis and pancreatitis with endotoxemia. A, Plasma levels of HRG were determined before treatment and 7, 24, and 48 hours after the first cerulein injection by western blotting. B, Quantification of the results of western blotting. *P < 0.05 vs sham. The results are presented as mean ± SEM of 4 mice. C, Mice were intraperitoneally injected with cerulein (100 μg/kg each) 7 times at 1-hour intervals, and LPS (5 mg/kg) was intravenously inj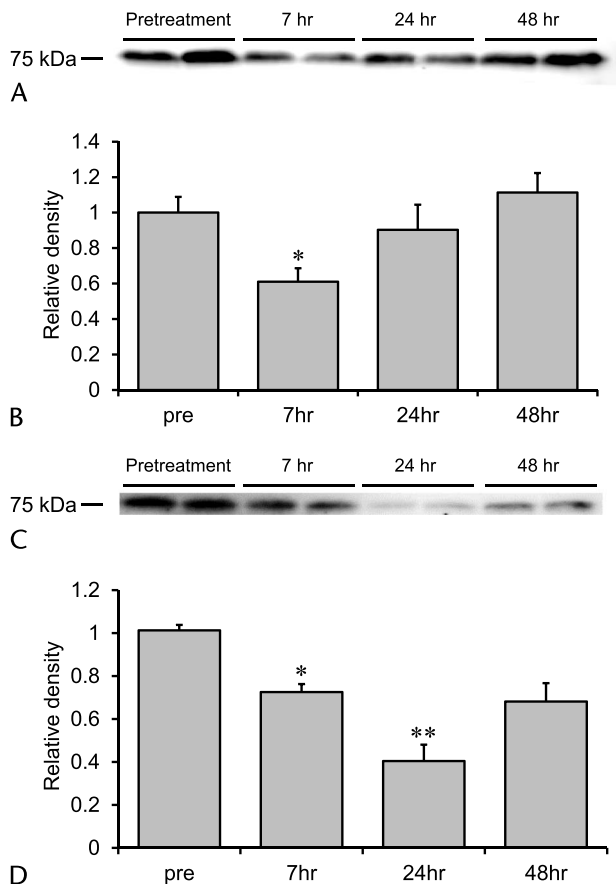ected 1 hour after the last cerulein injection. Plasma levels of HRG were determined before treatment and 7, 24, and 48 hours after the first cerulein ingestion by western blotting. D, Quantification of the results of western blotting. *P < 0.05 and **P < 0.01 vs sham. The results are presented as mean ± SEM of 4 mice.

Western Blot Analysis for HRG

Each 0.5 μL of plasma sample was electrophoresed on a polyacrylamide gel (10%) and transferred onto a polyvinylidene diflouride membrane (Bio-Rad, Hercules, Calif) for 150 minutes at 90 V. The membrane was then stained with SYPRO Ruby (Life Technologies, Carlsbad, Calif) and blocked with 20% skim milk for 60 minutes. The membrane was reacted with a rabbit-derived antihuman HRG polyclonal primary antibody (2.1 μg/mL) overnight at 4°C and washed 1 time with PBS. After washing, the membrane was reacted with peroxidase-labeled antirabbit IgG secondary antibody with 1000-fold dilution for 120 minutes at room temperature and washed 4 times with washing buffer. The bands were detected using Western blotting detection reagents (Pierce Biotechnology, Rockford, Ill).

Tissue Area/Total Area Ratio in Pancreas

Mice were killed 7, 24, or 48 hours after the first injection of cerulein. The pancreases were collected and fixed in 10% buffered formalin. The fixed pancreas was embedded in paraffin and sliced into 5-μm section. After hematoxylin-eosin (HE) staining, tissue area/total area ratio in pancreas was evaluated using ImageJ Version 1.51 (NIH, Bethesda, Md).

Statistical Analysis

All data were evaluated by one-way analysis of variance, followed by Dunnett test. The statistical differences between paired groups were determined using the Student's *t*-test. All data are presented as the mean ± standard error (SEM). *P* values of less than 0.05 were considered significant.

RESULTS

Condition of the Pancreas and the Plasma Levels of Pancreatic or Hepatic Enzymes in the Mouse Acute Pancreatitis Model

No animal died in the experimental period between the first injection and time of killing. At first, we used 5 mice for cerulein administration without the addition of LPS. The 7 hourly intraperitoneal injections of cerulein provoked severe pancreatitis at 7 hours after the first injection of cerulein. Degeneration of pancreatic acinar cells and extensive interstitial edema were observed by light microscopy (Figs. 1A, D). The histological damage gradually recovered thereafter. In the liver, the diffuse cell swelling was observed at 7 hours, which disappeared at 24 and 48 hours (Fig. 1B).

The serum concentrations of amylase and lipase increased markedly 7 hours after the first cerulein injection, at 3.6 and 6.9 times those of the pretreatment group, respectively (Fig. 1C). Likewise, the plasma concentrations of aspartate aminotransferase (AST) and alanine aminotransferase (ALT) were 4.6 and 5.9 times those of the pretreatment group, respectively (Fig. 1C).

Time-Series Variation of Plasma HRG Levels in Acute Pancreatitis With or Without Endotoxemia

Before, 7, 24, and 48 hours after the first injection of cerulein time-series variation of plasma HRG levels in acute pancreatitis with or without endotoxemia were performed in each 4 mice. The western blot analysis revealed changes in the plasma level of HRG at 7 hours after the first injection. The HRG level decreased to 61% of that in the intact animals. The level then
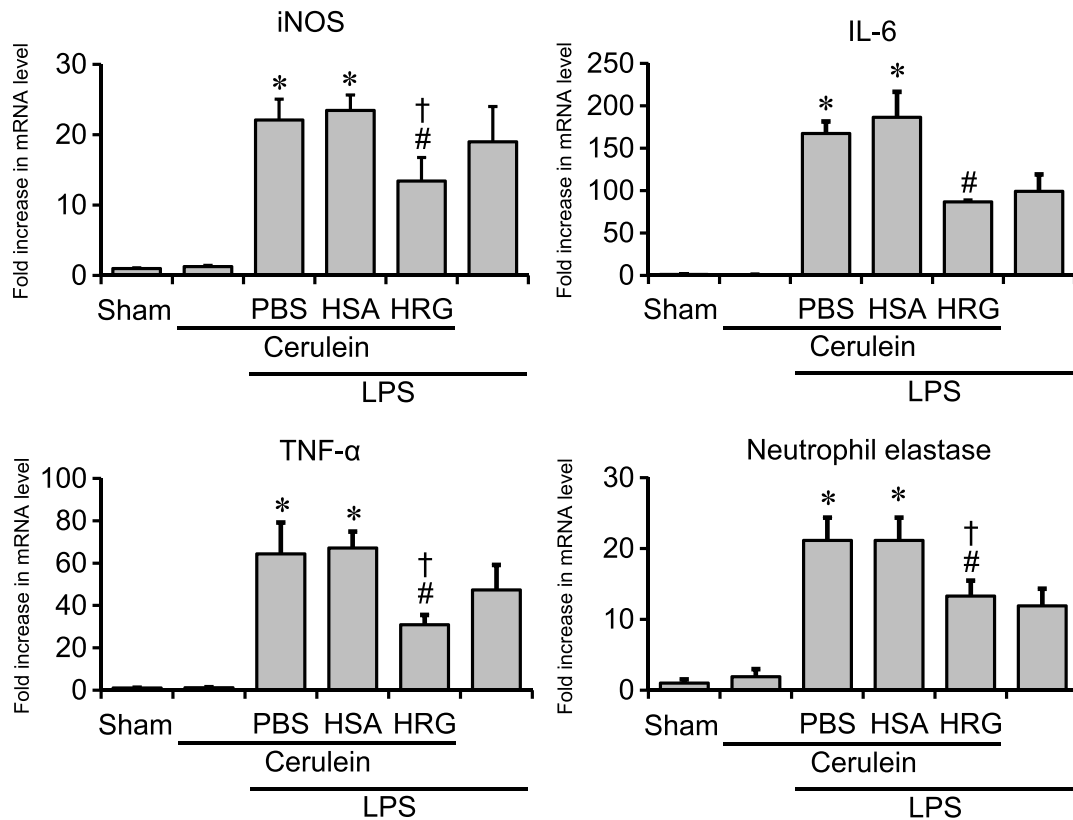

FIGURE 3. Determination of mRNA expressions in lungs. Lung samples for real-time PCR were collected 11 hours after the first cerulein injection. Relative expression levels of iNOS, IL-6, TNF-α, and neutrophil elastase were measured. *P < 0.05 vs sham, #P < 0.05 vs PBS, †P < 0.05 vs HSA. The results are presented as mean ± SEM of 6 mice.

recovered to the basal level 24 to 48 hours after the first cerulein injection (Figs. 2A, B). We did not observe lung injury in this animal model. The exogenous administration of HRG did not result in recovery of the damage in the pancreas. We therefore used an animal model of pancreatitis combined with LPS administration.

Seven hours after the first injection of cerulein, the HRG level decreased to 71% of that in the intact group. The level further decreased to 40% of the basal level 24 hours after the first injection, and it tended to recover thereafter (Figs. 2C, D).

The Effects of HRG on Lung Inflammation in Severe Acute Pancreatitis

Eleven hours after the first injection of cerulein, the treatment with cerulein alone did not change the expressions of mRNA of iNOS, IL-6, TNF-α, and neutrophil elastase compared with those of the sham group. The administration of LPS alone facilitated the expression of mRNA examined. The simultaneous administration of cerulein and LPS markedly increased the expression of mRNA, particularly IL-6 and neutrophil elastase mRNA. An injection of HRG immediately after the first cerulein injection reduced the
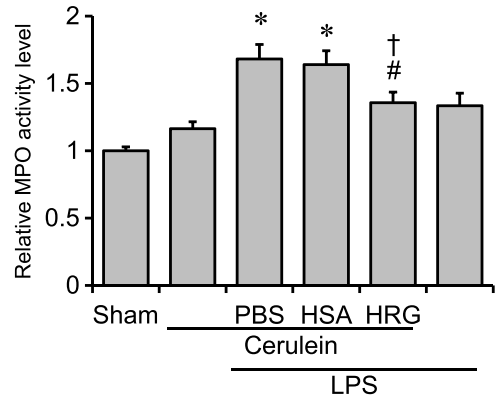

FIGURE 5. Effects of HRG on MPO activity. The MPO activity was measured in the lungs 24 hours after the first cerulein injection. *$P < 0.05$ vs sham, #$P < 0.05$ vs PBS, †$P < 0.05$ vs HSA. The results are presented as mean ± SEM of 11 mice.
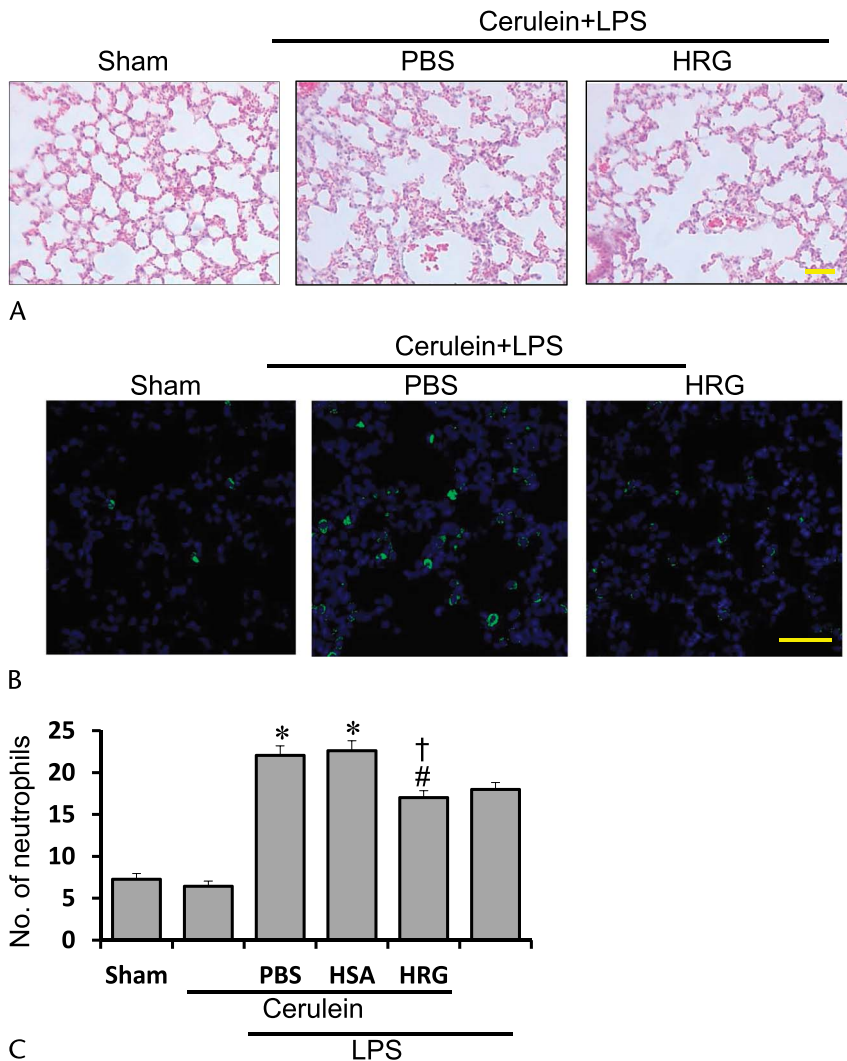

FIGURE 4. Typical photographs showing the lung by HE and Gr-1 stain 24 hours after the first cerulein injection. A, Lung section with HE stain 24 hours after the first of 7 injections of cerulein (100 μg/kg each). Scale bars, 50 μm. B, Neutrophils in the lung were stained by anti–Gr-1 antibody followed by fluorescence detection. Scale bars, 50 μm. C, The number of neutrophils was counted in each group. *$P < 0.05$ vs sham, #$P < 0.05$ vs PBS, †$P < 0.05$ vs HSA. The results are presented as mean ± SEM of 4 mice.

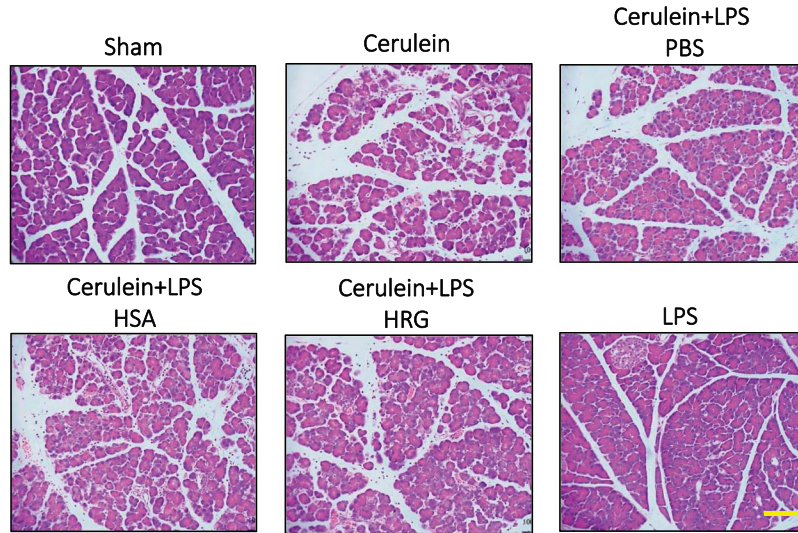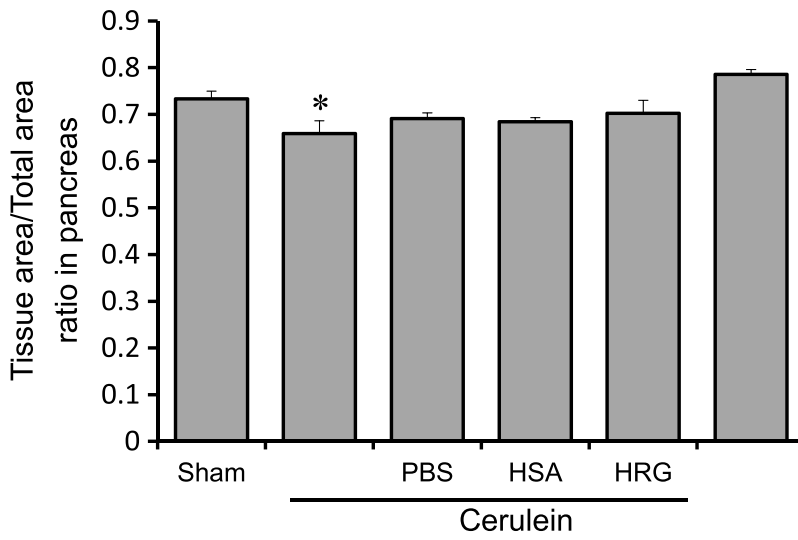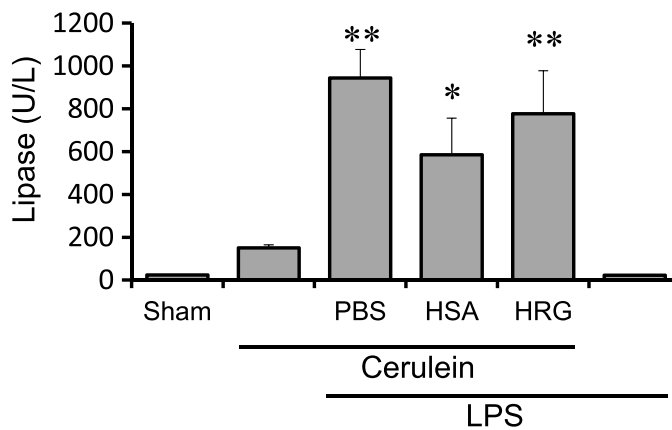**FIGURE 6.** Effects of HRG on pancreas in severe acute pancreatitis. A, Pancreas section with HE stain 24 hours after the first of 7 injections of cerulein (100 μg/kg each). Scale bars, 100 μm. B, Tissue area/total area ratio in pancreas was evaluated 24 hours after the first of 7 injections of cerulein (100 μg/kg each). *P < 0.05 vs sham. The results are presented as mean ± SEM of 5 mice. C, Serum concentrations of lipase at 24 hours after the first injection. *P < 0.05 and **P < 0.01 vs sham. The results are presented as mean ± SEM of 5 mice.

expression of mRNA, whereas the HSA treatment did not affect it (Fig. 3).

Twenty-four hours after the first injection of cerulein, the immunohistochemical staining for Gr-1 showed changes in the number of neutrophils similar to those in mRNA expression. Treatment with cerulein did not increase the number of neutrophils in the lung 24 hours after the first injection. An injection of LPS alone increased the neutrophil number. The addition of LPS to cerulein increased the number, although the extent of the increase was similar to that in the LPS-alone group. The HRG treatment decreased the number of neutrophils to 71%, whereas HSA did not suppress it (Figs. 4A–C).

A series of treatments with cerulein increased myeloperoxidase activity slightly 24 hours after the first injection, and the LPS injection alone facilitated it as well. The addition of LPS to the cerulein treatment markedly increased the myeloperoxidase activity. The HSA treatment suppressed the increased activity caused by both agents, whereas HSA showed no effects (Fig. 5).

The Effects of HRG on Pancreas and Liver in Severe Acute Pancreatitis

Histidine-rich glycoprotein did not significantly ameliorate the pancreatic damage when we observed the pancreatic tissue histologically at 24 hours after the first injection of cerulein (Figs. 6A, B). In addition, HRG did not reduce the activity of lipase in serum (Fig. 6C), suggesting the lack of effects of exogenous HRG on the severity on pancreatitis. In addition, HRG did not produce any significant effects on the liver injury judging from histological examination as well as serum transaminases (Figs. 7A, B).

DISCUSSION

We observed a decrease in the plasma HRG level in acute pancreatitis with or without endotoxin. The exogenous addition of HRG suppressed the increased activity of neutrophils as well as the expression of mRNA of proinflammatory cytokines.

The supramaximal stimulation of acinar cells by cerulein, a cholecystokinin analog, inhibits digestive enzyme secretion through cholecystokinin receptors. This leads to premature activation of digestive enzymes inside acinar cells, resulting in acute pancreatitis.[1,7] An imbalance between the production and secretion of these digestive enzymes is involved in the pathogenesis of acute pancreatitis.[1] When the production is excess relative to the secretion, the enzymes are released to systemic circulation, which increases the activities of amylase and lipase in the blood.[2] The degeneration of acinar cells, interstitial edema, and inflammatory cell infiltration that we observed in the present study are consistent with those reported in previous studies.[7,25] We observed that the plasma concentrations of AST and ALT were increased
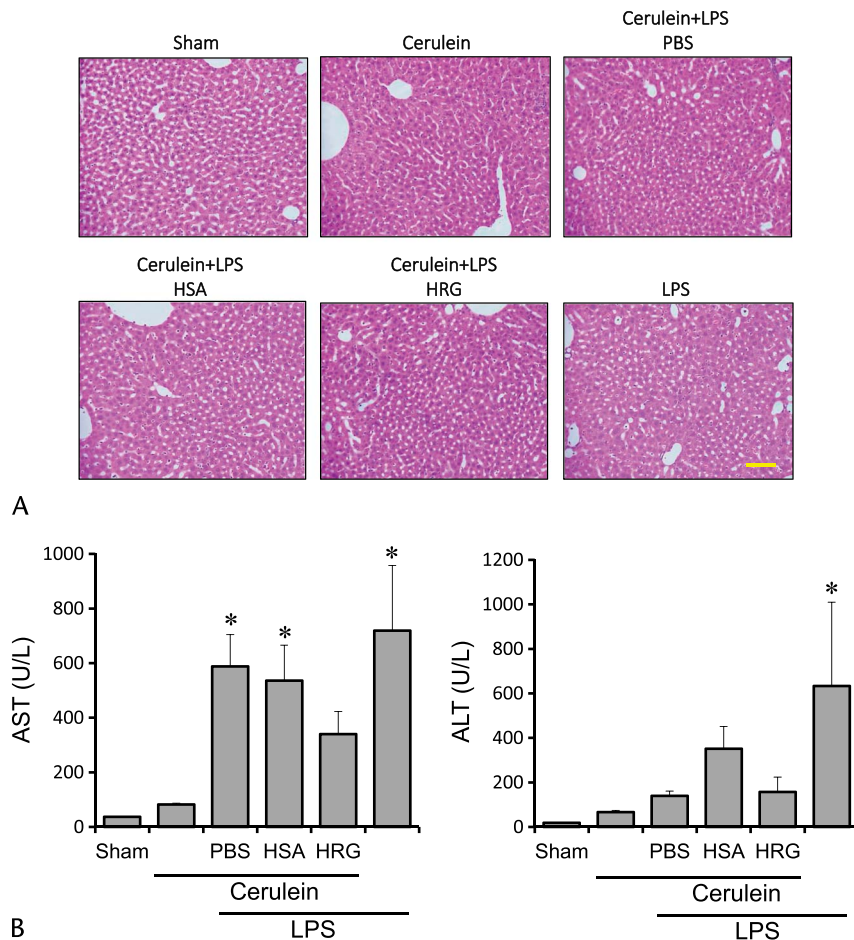

FIGURE 7. Effects of HRG on liver in severe acute pancreatitis. A, Liver section with HE stain 24 hours after the first of 7 injections of cerulein (100 μg/kg each). Scale bars, 100 μm. B, Serum concentrations of AST and ALT at 24 hours after the first injection. *P < 0.05 vs sham. The results are presented as mean ± SEM of 5 mice.

7 hours after the first injection of cerulein, as were those of amylase and lipase. Liver injury identified 7 hours after the first cerulein injection may be one of systemic complications or remote effects in this animal model.

The plasma concentration of HRG was decreased 7 hours after the induction of acute pancreatitis in this model. Similar findings were observed in our previous study, in which cecal ligation puncture was applied in mice.[6] The plasma concentration of HRG was decreased at 24 hours after puncture, and a supplemental administration of HRG inactivated neutrophil functions and ameliorated the prognosis of the septic animals.[6] The decrease in the HRG level was enhanced and sustained when an injection of LPS was added to this animal model of pancreatitis in the present study. Histidine-rich glycoprotein seems to be consumed to prevent the unnecessary activation of inflammatory cells in pancreatitis with infection.

In our previous study,[6] treatments of human neutrophils with 1 μM of HRG changed the shape of the neutrophils. The irregular surface became spherical in shape, and the diameter was shortened. Functional changes in adhesion and passage were also observed: suppression of adhesion on the vascular wall and a down-regulation of reactive oxygen species (ROS) production. Neutrophils treated with HRG readily passed through slits composed of capillaries, without being trapped. A loss of microvilli on the surface of neutrophils observed by scanning electron microscopy may be a mechanism underlying these morphological and functional changes in neutrophils.[6]

In the present investigation, we observed a decrease in the number of Gr-1–positive cells in the lung by HRG treatment. Likewise, the changes in MPO activity were in good agreement with those in the number of neutrophils. In an in vivo study, a depletion of peripheral neutrophils by antineutrophil antibody was effective to prevent lung injury caused by acute pancreatitis.[26] In that study, the antibody depressed both neutrophil infiltration and MPO activity.[26] Although the precise mechanism responsible for the decrease in the HRG level is unclear, the decreased activity of HRG may enhance the adhesion of neutrophils to microcapillaries in the lung, and the administration of HRG seems to prevent neutrophil toxicity to harm tissues.

We observed the lungs 24 hours after the first injection of cerulein. Considering that the expression of mRNA of neutrophil elastase was detected as early as that of proinflammatory cytokines, the activation of neutrophils seems to be rather rapid, and HRG suppressed the expression of mRNA of neutrophil elastase in the early phase.

The stimulation of cholecystokinin receptors generates ROS by NADPH oxidase, which produces proinflammatory cytokines and causes neutrophil recruitment and adhesion to capillary endothelial cells.[27] In addition to these inflammatory reactions, ROS plays a role in inducing apoptosis in pancreatic acinar cells.[28] Cerulein has been shown to promote DNA fragmentation mediated by an increase in the intracellular Ca^{2+} concentration.[29] However, the effects of HRG on apoptotic mechanisms remain unclear, as do the effects of HRG on mononuclear cells.

Because the present animal model well reflects general morphological features in acute pancreatitis, it is probable that HRG prevents the development of lung injury caused by acute pancreatitis. Considering that no treatment is currently available for progressive systemic inflammatory diseases, our findings regarding HRG may give rise to new ideas for therapeutic intervention.

ACKNOWLEDGMENTS

REFERENCES

1. Pandol SJ, Saluja AK, Imrie CW, et al. Acute pancreatitis: bench to the bedside. *Gastroenterology*. 2007;132:1127–1251.

2. Frossard JL, Steer ML, Pastor CM. Acute pancreatitis. *Lancet*. 2008;371:143–152.

3. Hartwig W, Werner J, Jimenez RE, et al. Trypsin and activation of circulating trypsinogen contribute to pancreatitis-associated lung injury. *Am J Physiol*. 1999;277:G1008–G1016.

4. Bhatia M, Brady M, Shokuhi S, et al. Inflammatory mediators in acute pancreatitis. *J Pathol*. 2000;190:117–125.

5. Levi M, Ten Cate H. Disseminated intravascular coagulation. *N Engl J Med*. 1999;341:586–592.

6. Wake H, Mori S, Liu K, et al. Histidine-rich glycoprotein prevents septic lethality through regulation of immunothrombosis and inflammation. *EBioMedicine*. 2016;9:180–194.

7. Matsuda N, Nishihira J, Takahashi Y, et al. Role of macrophage migration inhibitory factor in acute lung injury in mice with acute pancreatitis complicated by endotoxemia. *Am J Respir Cell Mol Biol*. 2006;35:198–205.

8. Zerem E. Treatment of severe acute pancreatitis and its complications. *World J Gastroenterol*. 2014;20:13879–13892.

9. Kylänpää ML, Repo H, Puolakkainen PA. Inflammation and immunosuppression in severe acute pancreatitis. *World J Gastroenterol*. 2010;16:2867–2872.

10. Chen HM, Shyr MH, Chen MF. Gabexate mesilate improves pancreatic microcirculation and reduces lung edema in a rat model of acute pancreatitis. *J Formos Med Assoc*. 1997;96:704–709.

11. Koide T, Foster D, Yoshitake S, et al. Amino acid sequence of human histidine-rich glycoprotein derived from the nucleotide sequence of its cDNA. *Biochemistry*. 1986;25:2220–2225.

12. Poon IK, Patel KK, Davis DS, et al. Histidine-rich glycoprotein: The Swiss Army knife of mammalian plasma. *Blood*. 2011;117:2093–2101.

13. Borza DB, Tatum FM, Morgan WT. Domain structure and conformation of histidine-proline-rich glycoprotein. *Biochemistry*. 1996;35:1925–1934.

14. Rydengård V, Olsson AK, Mörgelin M, et al. Histidine-rich glycoprotein exerts antibacterial activity. *FEBS J*. 2007;274:377–389.

15. Kacprzyk L, Rydengård V, Mörgelin M, et al. Antimicrobial activity of histidine-rich peptides is dependent on acidic conditions. *Biochim Biophys Acta*. 2007;1768:2667–2680.

16. Rydengård V, Shannon O, Lundqvist K, et al. Histidine-rich glycoprotein protects from systemic Candida infection. *PLoS Pathog*. 2008;4:e1000116.

17. Bosshart H, Heinzelmann M. Endotoxin-neutralizing effects of histidine-rich peptides. *FEBS Lett*. 2003;553:135–140.

18. Doñate F, Juarez JC, Guan X, et al. Peptides derived from the histidine-proline domain of the histidine-proline-rich glycoprotein bind to tropomyosin and have antiangiogenic and antitumor activities. *Cancer Res*. 2004;64:5812–5817.

19. Juarez JC, Guan X, Shipulina NV, et al. Histidine-proline-rich glycoprotein has potent antiangiogenic activity mediated through the histidine-proline-rich domain. *Cancer Res*. 2002;62:5344–5350.

20. Wake H, Mori S, Liu K, et al. Histidine-rich glycoprotein inhibited high mobility group box 1 in complex with heparin-induced angiogenesis in matrigel plug assay. *Eur J Pharmacol*. 2009;623:89–95.

21. Lijnen HR, Hoylaerts M, Collen D. Heparin binding properties of human histidine-rich glycoprotein. Mechanism and role in the neutralization of heparin in plasma. *J Biol Chem*. 1983;258:3803–3808.

22. Peterson CB, Morgan WT, Blackburn MN. Histidine-rich glycoprotein modulation of the anticoagulant activity of heparin. Evidence for a mechanism involving competition with both antithrombin and thrombin for heparin binding. *J Biol Chem*. 1987;262:7567–7574.

23. Leung LL. Interaction of histidine-rich glycoprotein with fibrinogen and fibrin. *J Clin Invest*. 1986;77:1305–1311.

24. Silverstein RL, Leung LL, Harpel PC, et al. Platelet thrombospondin forms a trimolecular complex with plasminogen and histidine-rich glycoprotein. *J Clin Invest*. 1985;75:2065–2073.

25. Grady T, Mah'Moud M, Otani T, et al. Zymogen proteolysis within the pancreatic acinar cell is associated with cellular injury. *Am J Physiol*. 1998; 275:G1010–G1017.

26. Inoue S, Nakao A, Kishimoto W, et al. Anti-neutrophil antibody attenuates the severity of acute lung injury in rats with experimental acute pancreatitis. *Arch Surg*. 1995;130:93–98.

27. Keck T, Friebe V, Warshaw AL, et al. Pancreatic proteases in serum induce leukocyte-endothelial adhesion and pancreatic microcirculatory failure. *Pancreatology*. 2005;5:241–250.

28. Yu JH, Kim H, Kim KH. Calcium-dependent apoptotic gene expression in cerulein-treated AR42J cells. *Ann N Y Acad Sci*. 2003;1010:66–69.

29. Yu JH, Lim JW, Kim KH, et al. NADPH oxidase and apoptosis in cerulein-stimulated pancreatic acinar AR42J cells. *Free Radic Biol Med*. 2005;39:590–602.